ADVANCING EARTH AND SPACE SCIENCES

Geophysical Research Letters

RESEARCH LETTER
10.1029/2023GL107991

Key Points:
- The new lifetime model provides extended space coverage in comparison to current widely used lifetime models
- Such parameterized lifetimes are very significant for simulations of the dynamics of radiation belt and ring current electrons
- Using the new electron lifetime model in simulations improves the agreement between the simulation results and the satellite observations

Supporting Information:
Supporting Information may be found in the online version of this article.

Correspondence to:
D. Wang,
dedong@gfz-potsdam.de

Citation:
Wang, D., Shprits, Y. Y., Haas, B., & Drozdov, A. Y. (2024). Improved lifetime model of energetic electrons due to their interactions with chorus waves. *Geophysical Research Letters*, *51*, e2023GL107991. https://doi.org/10.1029/2023GL107991

Received 21 DEC 2023
Accepted 3 SEP 2024

Improved Lifetime Model of Energetic Electrons Due to Their Interactions With Chorus Waves

Dedong Wang[1], Yuri Y. Shprits[1,2,3], Bernhard Haas[1,2], and Alexander Y. Drozdov[3]

[1]Section Space Physics and Space Weather, GFZ German Research Centre for Geosciences, Potsdam, Germany, [2]Institute of Physics and Astronomy, University of Potsdam, Potsdam, Germany, [3]Department of Earth, Planetary, and Space Sciences, University of California, Los Angeles, CA, USA

Abstract Chorus waves induce both electron acceleration and loss. In this letter, we provide significantly improved models of electron lifetime due to interactions with chorus waves. The new models fill the gap that previous models have on some magnetic local time (MLT) sectors of the Earth's magnetosphere. This improvement is critical for modeling studies. The lifetime models developed using two different methods are valid for electrons with an energy range from 1 keV to 2 MeV. To facilitate the integration of these new models into different ring current and radiation belt codes, we parameterize the electron lifetime as a function of *L*-shell and electron kinetic energy at each MLT and geomagnetic activity (Kp). The parameterized electron lifetimes exhibit strong dependencies on *L*-shell, MLT, and energy. Simulations using these new models demonstrate improved agreement with satellite observations compared to simulations using previous models, advancing our understanding of electron dynamics in the magnetosphere.

Plain Language Summary There are a large number of energetic electrons trapped by our Earth's magnetic field in the near-Earth space. The regions populated by these high energy electrons are called ring current and radiation belts. It is important to understand the dynamics of the energetic electrons because they can be dangerous to satellites and astronauts flying through these regions. Electromagnetic waves in these regions play an important role in the dynamic of ring current and radiation belt electrons. Among these waves, whistler mode chorus wave is an important wave that can cause both acceleration and loss of the energetic electrons. In our previous studies, we calculated diffusion coefficients to quantify the effect of chorus waves on the energetic electrons. Based on these diffusion coefficients, in this study, we estimate the lifetime of energetic electrons due to their interactions with chorus waves. To make this lifetime model more convenient to be used in different ring current and radiation belt models, we apply polynomial fits to the calculated lifetime. Our new lifetime model is more advanced than previous models, especially in the space coverage. We test the new models in simulations and the results agree better with satellite observations than the previous models do.

1. Introduction

The energetic electrons in the Earth's outer radiation belt and ring current can be very dynamic and show a very strong dependence on the geomagnetic conditions. The flux of the energetic electrons can vary by several orders of magnitude in the time scale of days to hours, especially during geomagnetic storms (e.g., Reeves et al., 2003). Wave-particle interactions play an important role in the dynamic evolution of the energetic particles. In particular, chorus waves can cause both energy and pitch-angle diffusion of energetic electrons (e.g., Millan & Baker, 2012; Shprits et al., 2008; Thorne, 2010). Diffusion in pitch-angle can transport electrons into their loss cones, where they collide with atmospheric particles and are lost from the inner magnetosphere. Outside the plasmasphere, pitch-angle scattering by chorus waves is one of the dominant loss mechanisms of high-energy electrons (e.g., Albert, 2005; Horne & Thorne, 2003; Thorne et al., 2005). Quasi-linear diffusion coefficients can be calculated to quantify these processes, using statistical global distribution of chorus waves (e.g., Albert, 2005; Glauert & Horne, 2005; Shprits, Thorne, et al., 2006; Summers, 2005; Wong et al., 2024; Zhu et al., 2019). Diffusion coefficients can be used to simulate the dynamics of energetic electrons by solving the 3-dimensional (3D) Fokker-Plank equation. Here, the 3D diffusion means diffusion in radial, pitch-angle (PA) and momentum (energy) dimensions with mixed PA-energy diffusion. However, full 3D diffusion simulations are computationally expensive and may pose challenges for certain applications, such as real-time nowcasting. Furthermore, if the focus of a study is the precipitation caused by chorus waves, full 3D diffusion is not necessarily needed. In this situation, electron lifetimes computed based on bounce-averaged quasi-linear diffusion coefficients (e.g., Albert

& Shprits, 2009; Glauert et al., 2024; Gu et al., 2012; Orlova & Shprits, 2014; Shprits et al., 2007) can be used. The term "lifetime" is not only used to describe the decay time of trapped particles, but also useful to calculate precipitation of them.

Before the launch of the Van Allen Probes mission, the global distribution of chorus waves was provided by the measurements from several satellite missions, for example, the Combined Release and Radiation Effects Satellite (CRRES) mission, the Time History of Events and Macroscale Interactions during Substorms (THEMIS) mission, the Cluster mission and the Polar satellite. Some chorus wave models have been developed by using data from CRRES (e.g., Li et al., 2007; Meredith et al., 2003; Meredith et al., 2004). Based on these models, Shprits et al. (2007) calculated lifetime of electrons with energies between 100 keV and 2 MeV. In that study, they considered lower-band chorus waves in the magnetic local time (MLT) region of 0,600–1,500. Based on observations from CRRES, THEMIS satellites (Li et al., 2009, 2011), Polar satellite (Bunch et al., 2011), and simulation studies (Ni et al., 2011a, 2011b), Gu et al. (2012) extended the energy range of parameterized electron lifetimes to 1 keV - 2.0 MeV by taking oblique lower-band and upper-band chorus waves into account. The chorus wave parameters in Gu et al. (2012) are taken from those studies under geomagnetic active conditions and then scale to other geomagnetic conditions with magnetic intensity following Subbotin et al. (2010). Using the chorus wave model developed by Spasojevic and Shprits (2013), Orlova and Shprits (2014) computed lifetimes of 1 keV–2 MeV electrons in 4 MLT sectors. These parameterizations of wave models and electron lifetimes have been widely adopted in many radiation belt modeling works (e.g., Drozdov et al., 2017, 2021; Kim et al., 2012; Ozeke et al., 2018; Ripoll et al., 2016; Shprits et al., 2009; Subbotin et al., 2011; Xiao et al., 2009), and the simulation results have shown reasonable agreement with the electron fluxes observed by satellites. Recently, Aseev et al. (2019) and Haas et al. (2022) performed simulation for ring current electrons using the electron lifetime provided by Gu et al. (2012) and Orlova and Shprits (2014), respectively, to account for the electron loss caused by chorus waves. However, these electron lifetime models have gaps in MLT. It is necessary to make some assumptions of lifetime in those MLT gaps.

Using more than 5 years of Van Allen Probe data, which covered all MLTs, Wang et al. (2019) developed chorus wave models with MLT, L (approximately the distance from the center of the Earth at the geomagnetic equator, normalized by the Earth radii), geomagnetic latitude and Kp dependence. However, the maximum geomagnetic latitude of the chorus wave models from Wang et al. (2019) is 20°, due to the orbit limitation of Van Allen Probes. Referring to observations from the Cluster satellites (Agapitov et al., 2018), Wang and Shprits (2019) extended the chorus wave models to high latitudes and showed that chorus waves at high latitudes play an important role in the loss of MeV electrons by calculating diffusion coefficients (see details in Text S1 in Supporting Information S1) and performing 1 year long-term 3-dimensional (3D) Fokker-Plank simulation. Using these diffusion coefficients, Wang et al. (2020) performed 3D simulations for the radiation belt dynamics for different challenge events selected by the U.S. National Science Foundation's Geospace Environment Modeling (GEM) focus group "Quantitative Assessment of Radiation Belt Modeling" (Tu et al., 2019). The 3D simulation has been extended for several years during the Van Allen Probe era (Shprits et al., 2022, see their Figure 27). The simulation results agree well with satellite observations. The electron lifetime model presented in this paper offers a significantly simpler way of taking into account the loss of energetic electrons caused by chorus waves, for simulating radiation belt and ring current dynamics. The MLT dependence of trapped electrons with energies higher than several hundred keV can be small. However, their precipitation is still MLT-dependent, which is one of the important reasons that we need to develop MLT-dependent electron lifetime models. Accurate simulation of MLT-dependent precipitation is important for the study of magnetosphere-ionosphere coupling. In Section 2, using the quasi-linear diffusion coefficients which has been validated by several studies (Shprits et al., 2022; Wang et al., 2020; Wang & Shprits, 2019), we calculate the lifetime of electrons due to their interaction with chorus waves. To facilitate the usage of our model in 4-D convection or particle tracing codes, in Section 3, we parameterize the lifetimes using regression and polynomial fit following previous studies (Gu et al., 2012; Orlova & Shprits, 2014; Shprits et al., 2007). Table S1 in Supporting Information S1 briefly summarizes these previous and current efforts of lifetime parameterization due to interaction with chorus waves. We compare the parameterized electron lifetime caused by the chorus waves from our current study and previous studies in detail in Section 4. Simulations using different lifetime models have been performed. We validate the simulation results against the satellite observations. Section 5 discuss the limitations and caveats of the electron lifetime approach. Section 6 summarizes our current work.

2. Methods

2.1. Estimation of Electron Lifetimes

Shprits, Li, and Thorne (2006) showed that when the pitch-angle diffusion coefficient (as a function of the equatorial pitch-angle, α) has no pronounced local minima below 1/10th of the pitch-angle diffusion coefficient near the edge of the loss cone, the pitch-angle distribution of phase space density decays exponentially with the same rate at all equatorial pitch-angles, preserving the shape of the distribution function (see Figure S1 in Supporting Information S1). In this situation, the approximate lifetimes of the electrons can be evaluated as:

$$\tau_{LC} = \frac{1}{D_{\alpha\alpha}(\alpha_{\mathrm{LC}})}, \tag{1}$$

where $D_{\alpha\alpha}(\alpha_{LC})$ is the bounce-averaged pitch-angle diffusion coefficient at the edge of the loss cone. In a dipole field assumption, an approximation of the equatorial loss cone can be given by

$$\alpha_{\mathrm{LC}} = \arcsin \frac{L^{-\frac{3}{2}}}{(4-3/L)^{\frac{1}{4}}}\ (\mathrm{rad}) \tag{2}$$

at a specific L.

Black lines in Figure 1 show examples of pitch-angle diffusion coefficients as a function of equatorial pitch-angle for electrons at 0.9 MeV and Kp = 3, L = 5 in different MLTs (MLT = 6, 9, 12, 15 in panels a–d, respectively). The pitch-angle diffusion coefficient profiles at MLT 6 (panel a) and 9 (panel b) exhibit minima at intermediate pitch-angles, which are labeled using red dots in these panels. The pitch-angle diffusion coefficients at MLT 12 (panel c) and 15 (panel d) have minimum value near the 90° equatorial pitch-angle. The chorus waves on the dayside and the duskside have less power near the equator than those at higher latitudes (Wang et al., 2019). Thus, the pitch-angle diffusion coefficients are significantly smaller for electrons trapped near the equator on the dayside and duskside. In Figure 1, the loss cone pitch-angles are highlighted using a red vertical line in each panel. To compare $D_{\alpha\alpha}(\alpha_{LC})$ with the local minima $D_{\min}$ at intermediate pitch-angles, we plot $D_{\alpha\alpha}(\alpha_{LC})$ using "+" marker at the pitch-angle where the local minima exists in panels (a) and (b) of Figure 1. In Figure 1a, $D_{\alpha\alpha}(\alpha_{LC})$ indicated by + is very close to $D_{\min}$ indicated by the red dot. In Figure 1b, they are in the same order of magnitude. In Figures 1c and 1d, where $D_{\min}$ are close to 90°, we plot $D_{\alpha\alpha}(\alpha_{LC})$ at intermediate pitch-angles.

Albert and Shprits (2009) investigated the situation where pitch-angle diffusion coefficients have a deep minimum at some equatorial pitch-angle (α_*). They show that in this situation the electron lifetime (τ_*) can be estimated as

$$\tau_* \equiv \int_{\alpha_{\mathrm{LC}}}^{\pi/2} d\alpha \frac{\cos\alpha}{2D_{\alpha\alpha}\sin\alpha}. \tag{3}$$

This formula suggests that the lifetime will be determined mostly by the minimum value of $2D_{\alpha\alpha}\tan\alpha$. Blue lines in Figure 1 show $D_{\alpha\alpha}\times\tan\alpha$. We calculated $1/\tau_*$ and show them as green circles in Figure 1. It can be seen that, when the local minima is not deep, the differences between τ_{LC} indicated by "+" and τ_* (green circles) are not significant, as shown in Figures 1a–1c. This is consistent with Albert and Shprits (2009), who found that the τ_{LC} is a good approximation of electron lifetime for small and moderate step minima. It only breaks down when the step minima is smaller than $\frac{1}{10}D_{LC}$ and wide enough (~40° width), which is the case in Figure 1d. In this situation, the pitch-angle diffusion coefficients near the 90° are so small that the corresponding electrons practically do not diffuse. As a result, the equilibrium pitch-angle distribution cannot be reached only by interactions with chorus waves at this MLT. The lifetime calculated using Equation 3 in this case is longer than 100 days (the inversion of the value indicated by the green circle), while the lifetime estimated using Equation 1 is several days. However, there can be other waves in space that the particles encounter (e.g., magnetosonic waves) or other mechanisms (e.g., bounce resonance) which can cause the diffusion of electrons near 90° pitch-angle.

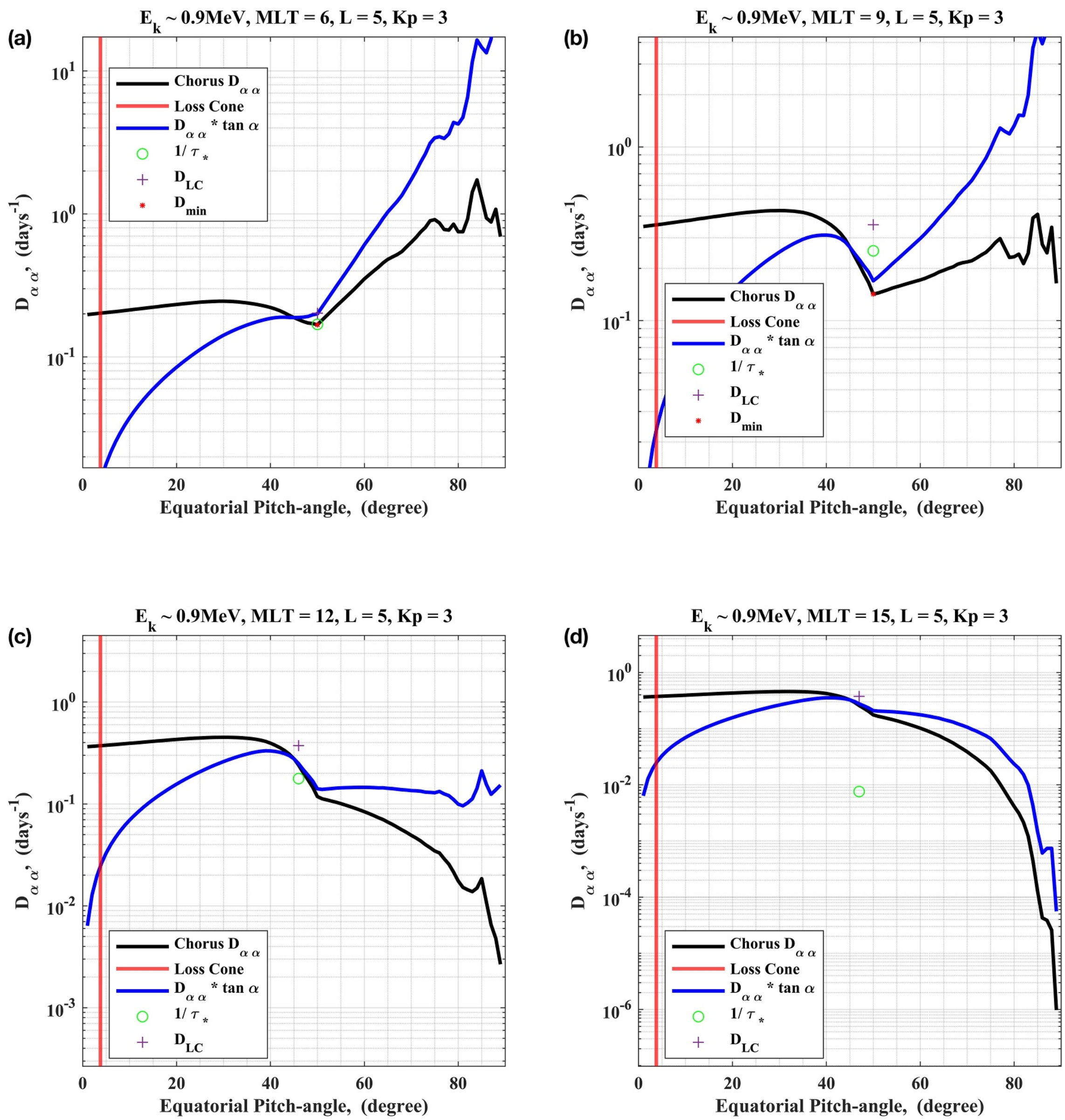

Figure 1. The four panels in this figure share the same format. The x-axis of each panel shows the equatorial pitch-angle with the unit degree. The y-axis shows the pitch-angle diffusion coefficients. Panels (a)–(d) show diffusion coefficients at different MLTs (6, 9, 12, 15) for electrons with energy near 0.9 MeV, at $L = 5$ and Kp = 3. Black lines in each panel show the pitch-angle diffusion coefficients, while blue lines show diffusion coefficients multiplied by $\tan \alpha$. Loss cone angle are indicated by the red vertical lines. We also show diffusion coefficients near the loss cone (D_{LC}), the inverse of estimated life time (τ_*) using Equation 3, and the minima (D_{min}) in the pitch-angle diffusion coefficient profile in the intermediate pitch-angle.

2.2. Strong Diffusion Limit

Electrons with pitch angles smaller than the loss cone ($\alpha_{eq} < \alpha_{lc}$) will be lost on average a quarter of their bounce period τ_B. In the strong diffusion regime, the speed of the particles coming into their loss cones is comparable or even faster than their atmospheric loss rate. The calculated lifetime should not be shorter than the lifetime in the strong diffusion limit. We compare the calculated electron lifetime with the strong diffusion limit $\tau_{\mathrm{SD}} = 1/D_{\mathrm{SD}}$ defined by Kennel (1969). The strong diffusion coefficient (D_{SD}) is reasonably given by Summers and Thorne (2003) as follows:

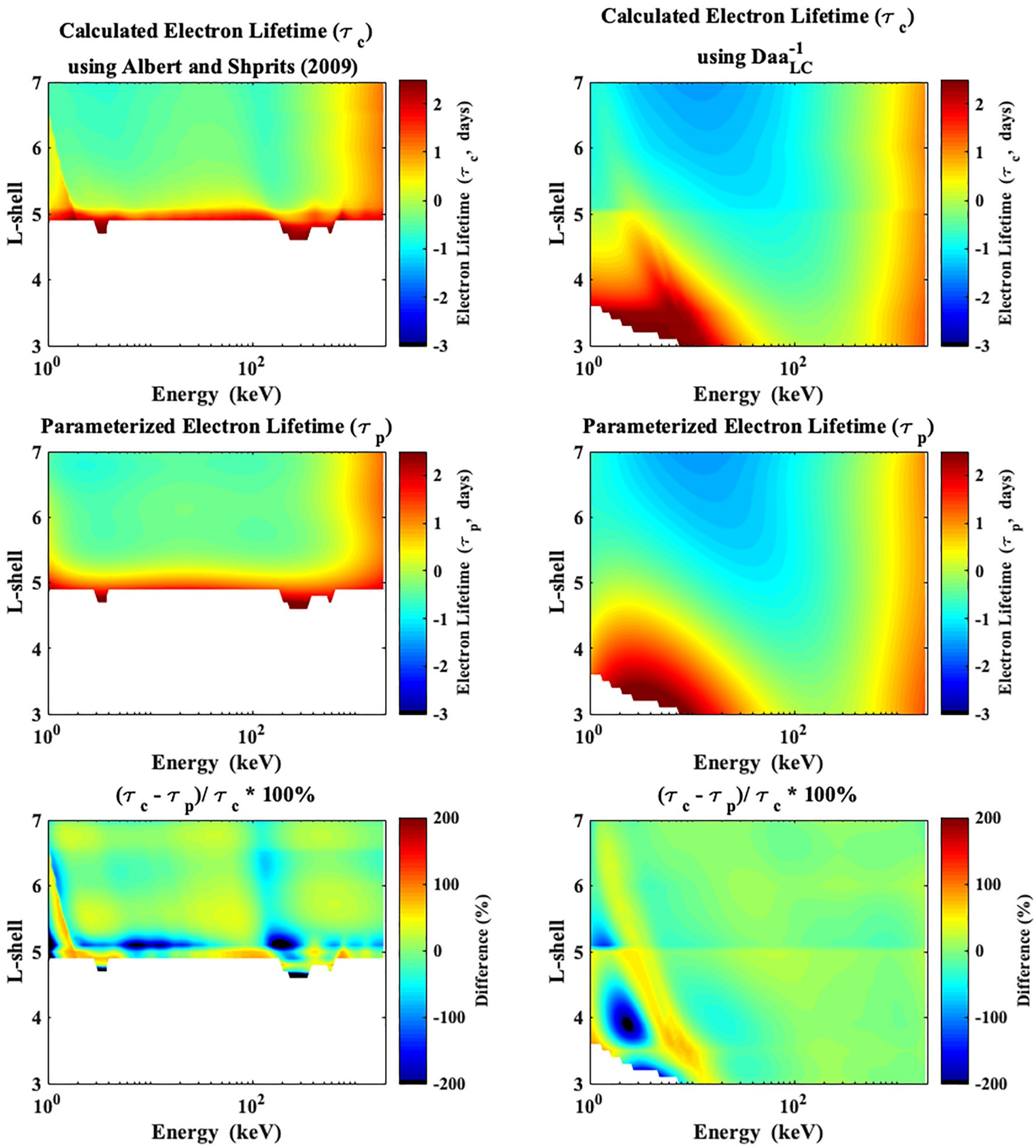

Figure 2. The electron lifetime caused by chorus waves at MLT = 15 and Kp = 4. The six panels in this figure have the same format. The *x*-axis of each panel shows the kinetic energy of electrons. The *y*-axis shows *L*−shell value. Colorbars in the top four panels show the electron lifetime in the unit of days. Panels in the first row show calculated electron lifetime using two different methods in two columns. Panels in the second row show the parametrized electron lifetime. Panels in the third row show the normalized difference between the calculated and parametrized electron lifetime.

$$D_{\mathrm{SD}} \approx \frac{9.66}{L^4}\left[\frac{4L}{4L-3}\right]^{\frac{1}{2}}\frac{[E(E+2)]^{\frac{1}{2}}}{E+1}(s^{-1}), \tag{4}$$

where $E = E_k/m_e c^2$ is the kinetic energy with unit of its rest energy $m_e c^2$. We calculate the strong diffusion limit $\tau_{\mathrm{SD}} = 1/D_{\mathrm{SD}}$. When the calculated lifetime is shorter than the lifetime predicted by the strong diffusion, we replace the calculated lifetime with the lifetime predicted by the strong diffusion. Two examples of the final electron lifetime that we obtained in this section are color-coded in the panels in the first row of Figure 2. The *x*-axis of these panels are the kinetic energy of electrons in the unit of keV. The *y*-axis of these panels are the L-shell.

We show electron lifetime at Kp = 4 and MLT = 15. The left column shows the electron lifetime calculated using Equation 3, while the right column shows the electron lifetime calculated using Equation 1. Lifetimes longer than 300 days are not shown since such long lifetime leads to negligible losses. Comparing these two panels, we can see that at MLT = 15, the lifetime calculated using the two methods are significantly different, which is consistent with Figure 1d. We can also see that the electron lifetime has a strong dependence on L and energy of electrons. In particular, the lifetimes for electrons with lower energy (<100 keV) range from hours at higher L ($L > 5$) to days at lower L ($L < 5$). In the heart of the radiation belt ($L \approx 4$), the lifetime calculated using Equation 1 varies from hundred days for electrons at tens of keV to several hours for electrons at 100–300 keV. During this storm time (Kp = 4), the lifetimes for higher energy >100 keV electrons range from hours at 100–300 keV to days for electrons with energy higher than 500 keV.

3. Electron Lifetime Parametrizations

The complete electron lifetime dataset provided in the last section can certainly be used to conduct a simplified simulation. However, it requires the matching of the tabular data with the simulation grid. To provide a convenient form of calculated electron lifetime, and to investigate the functional dependence of the electron lifetime on the electron kinetic energy and $L-$shell value, we parametrize the electron lifetime as a function of them at each MLT and Kp. The coefficients of the parameterized equations are derived using the linear regression technique in a similar way as in Shprits et al. (2007) and Gu et al. (2012). Panels in the second row of Figure 2 illustrate the parameterized lifetime at MLT = 15 and Kp = 4. In general, the parameterized lifetimes agree well with the calculated lifetimes. To quantify the difference between them, we calculate the difference between the calculated lifetime and the parameteried lifetime, but normalized by the calculated lifetime, which is shown in the panels in the third row of Figure 2. In the left column of Figure 2, the accuracy of the parameterization is within 50% above L = 5.5 for electrons with energy from 3 to 100 keV and from 300 keV to MeV. In the right column, for energies higher than 20 keV at $L < 5$ and for energies higher than several keV at $L > 5$, our parameterization is accurate to within 50%. The error is very low compared to the inaccuracy from uncertainties associated with wave models and electron density models (Shprits et al., 2007).

4. Comparison With Previous Parametrization of Electron Lifetime Caused by Chorus Waves

In comparison with previous studies that have provided the electron lifetime due to interactions with chorus waves (e.g., Gu et al., 2012; Orlova & Shprits, 2014; Shprits et al., 2007), our current research stands out in one significant way: it extends the model to cover the afternoon to dusk side. This sector was not addressed before due to the limitation of the wave measurements and data availability. Figure 3 shows an example of comparing the parameterized lifetime by this study with two methods (panels (c) and (d)) and previous studies (panel (a) from Gu et al. (2012) and panel (b) from Orlova and Shprits (2014)) for electrons with an energy at 50 keV and when Kp = 5. In Figure 3, the Sun is to the left and we are looking down at the Earth from the north pole. The electron lifetime is color-coded in these dial plots in a logarithmic scale in the unit of days. The inner boundary of these color-coded plots are at 3 Earth Radii (R_E) from the center of the Earth, and the outer boundary at 6 R_E. Figure 3a shows that the electron lifetime model provided by Gu et al. (2012) covers MLT from 0 to 12. Figure 3b shows that the electron lifetime model provided by Orlova and Shprits (2014) covers MLT regions from night side to the noon sector, but still has a gap in the dusk to evening sector. The electron lifetime model provided by this study shown in Figures 3c and 3d covers all the MLT regions, which is a significant improvement comparing with those previous electron lifetime models. In general, the electron lifetime in the MLT sectors covered commonly by these models agree well with each other. In the dusk to evening sectors, electron lifetime provided in this study but calculated using two methods differ from each other. The reason is that, in these MLT sectors, the diffusion coefficients have minimum values near 90° pitch-angle, which results in larger calculated electron lifetime following Equation 3 but does not influence lifetime estimated using Equation 1.

To test the effect of the different electron lifetime models, we have performed simulations for ring current electrons with energies at 10 s of keV using the four dimensional Versatile Electron Radiation Belt (VERB-4D) code (Shprits et al., 2015). We performed simulations for a relatively geomagnetically quite period (see Figure 4a) in order to eliminate the uncertainties from convection electric field model during geomagnetic storms. For the full description of the VERB-4D model and the exact setup of the simulations, we refer to previous work (Haas et al., 2023) and Text S2. Figure 4 presents the results of the simulations using all four electron lifetime models

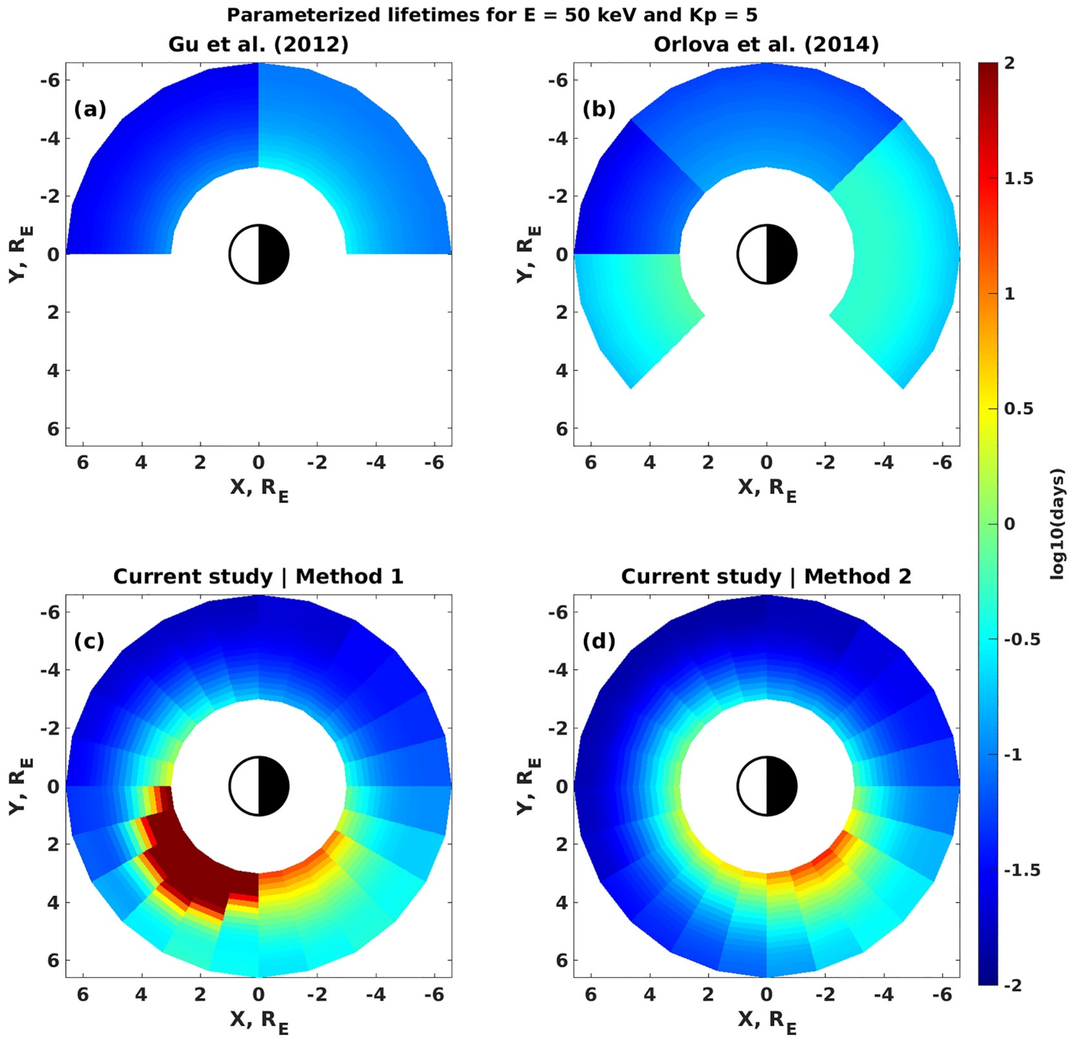

Figure 3. An example of comparing the parametrized lifetime provided by current study with two different methods and previous studies, for electrons with kinetic energy at 50 keV and at Kp = 5. The inner boundary of these color-coded plots are at 3 Earth Radii (R_E) from the center of the Earth, and the outer boundary at 6 R_E. The Sun is to the left and we are looking down at the Earth from the north pole. Panel (a) shows the results from the electron lifetime model from Gu et al. (2012). Panel (b) shows the electron lifetime provided by Orlova and Shprits (2014). Panel (c) illustrates the parameterized electron lifetime from this study. The method of calculating electron lifetime from diffusion coefficients is following Albert and Shprits (2009). Panel (d) depicts the electron lifetime provided by this study. The electron lifetime used in this panel is calculated from the same diffusion coefficients as those in panel (c) but using the method provided by Shprits et al. (2007).

(Gu et al. (2012); Orlova and Shprits (2014), and electron lifetime using method 1 and 2 in this study). We validate our simulation results against observations from RBSP-B satellite. Figure 4b shows the distance of RBSP-B from the center of the Earth in R_E. Panels c–e show the observed flux (black line) and simulated flux (other colors) for electrons at 10 keV, 25 and 50 keV. We calculated the root mean square error (RMSE) to validate the simulation results against observations and they are shown with the color-coded texts in the panels. From these values we can see that the simulations using the electron lifetime models developed in this study agree better with the observation. This shows that the electron lifetime models developed in this study should be used in future simulation studies.

5. Discussions and Caveats

Please note that the lifetime model provided in this paper is dedicated to describe the important precipitation loss caused by chorus waves. To model the total loss of energetic electrons, contributions of other waves need to be

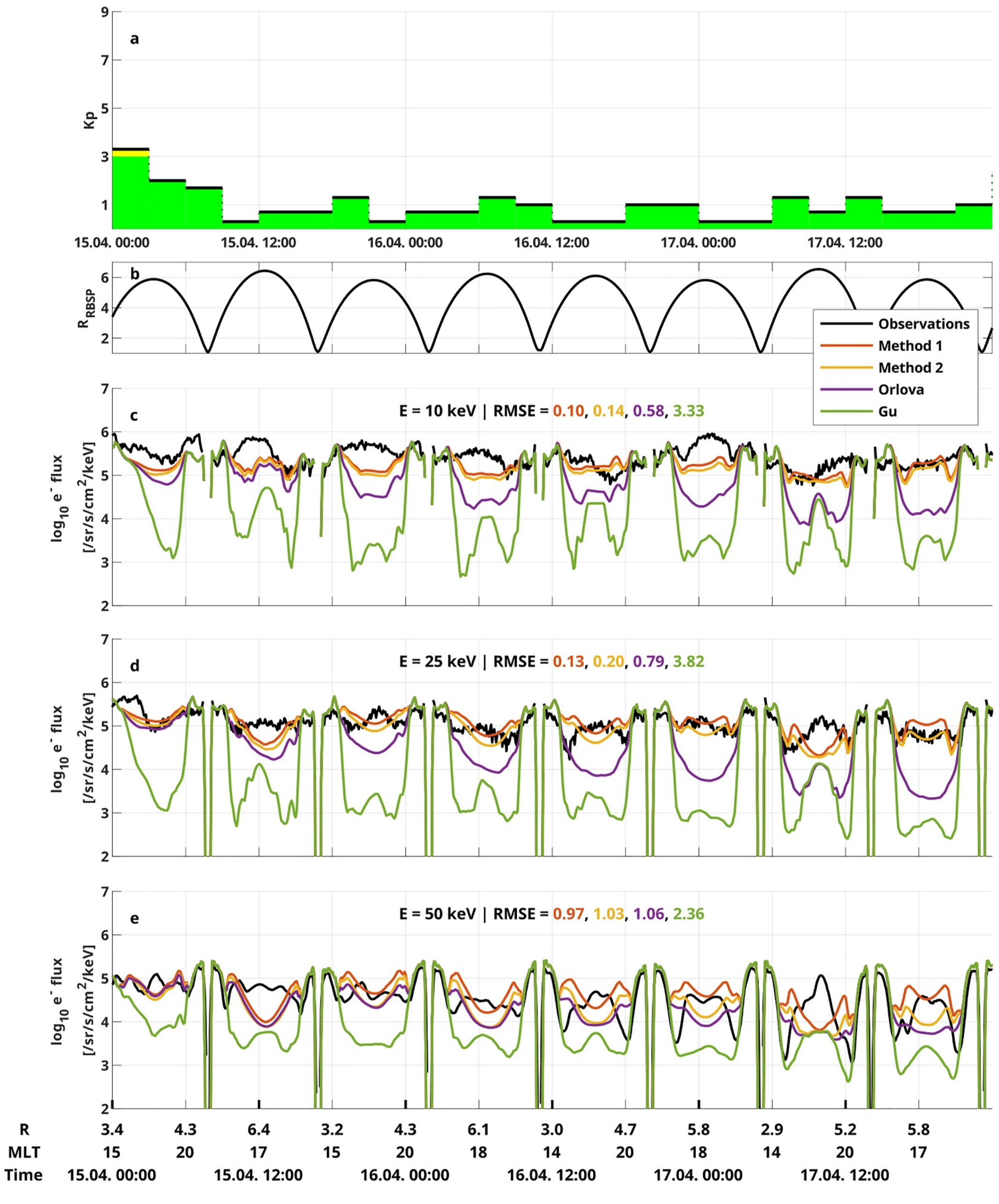

Figure 4. (a) Geomagnetic index Kp from April 15 to 17 April 2017. (b) The distance of RBSP-B from the center of the Earth but normalized by the Earth radii (R_E). (c)–(e) The observed flux (black line) by RBSP-B and simulated flux by VERB-4D (other colors) for electrons at 10 keV, 25 and 50 keV.

included. In the simulations shown in Figure 4, loss induced by hiss waves has been included using the lifetime model due to interaction with hiss waves referring to Orlova et al. (2016). Effects of EMIC waves are not included in this particular simulation because here we focus on electrons at relatively lower energies ($\leq$ 50 keV) while effects of EMIC waves on electrons at these energies are not significant (e.g., Shprits et al., 2022; Wang et al., 2020).

Here we also discuss the caveats of the lifetime approach. It is a standard concept that long-time pitch angle diffusion toward the loss cone leads to exponential decay as shown in Figure S1 in Supporting Information S1 and previous literature (e.g., Shprits et al., 2008). For 10 s of keV ring current electrons, this exponential decay time can be comparable with their drifting time in each MLT sector if one compares the lifetime calculated in each

MLT sector shown in Figure S1 in Supporting Information S1 and the drifting time shown in Figure S2 in Supporting Information S1. But the lifetime approach only captures the slowest timescale of the diffusion operator; it ignores the relaxation to the lowest eigenmode, which is especially important if the goal is to capture rapid, drift-resolved dynamics. It also ignores energy diffusion, which is a crucial part of chorus waves acting on electrons. We have performed simulation tests using the lifetime approach and the full diffusion approach. Figures S3-S6 in Supporting Information S1 compare the results. Details of the code description, simulation set up and related discussion can be found in Text S2, S3. The lifetime approach can reasonably calculate the precipitation flux but may underestimate the trapped particles. Trapped electrons with higher energies can drift faster than the time scale of PA diffusion. For electrons with energy higher than 200 keV, the trapped population doesn't show MLT dependence. However, the MLT-dependent lifetime is not only for the calculation of trapped electrons, but also for the precipitation of energetic electrons, which show MLT dependence even at MeV energies.

We calculate the electron lifetime due to their interactions with upper- and lower-band chorus waves based on the quasi-linear theory using empirical wave and plasma density models (Sheeley et al., 2001; Wang et al., 2019). There are some studies comparing the classical quasi-linear diffusion coefficients and those calculated using test particle codes. For example, Tao et al. (2011) followed the trajectories of a large number of electrons in a numerically constructed, broadband, small-amplitude wave field, using a general relativistic test particle code. Their results showed the change in pitch angle and energy of each electron was stochastic and the resulting diffusion of the entire population was in excellent agreement with quasi-linear theory. Recently, using test particle simulations, Cai et al. (2020) investigated the effects of nonlinear resonance broadening on interactions between whistler mode waves and energetic electrons for the first time. They found that resonance broadening effects are important for large pitch angles near 90°. Thus, diffusion coefficients calculated from test particle simulations may be different from those calculated using quasi-linear theory only at large pitch-angles. As a result, only those lifetime evaluated following Albert and Shprits (2009) will be influenced because Equation 3 take into account diffusion coefficients at large pitch-angles, while the electron lifetime evaluated following Shprits et al. (2007) will not be influenced because the diffusion coefficients near the loss cone is similar using quasi-linear theory and test particle simulations.

6. Summary

In this paper, we present the updated global electron lifetime based on recent chorus wave models from the Van Allen Probe observations (Wang et al., 2019) and assumptions of the chorus wave distribution at high latitudes following Wang and Shprits (2019). These assumptions are referred to chorus wave observations from the Cluster satellite (Agapitov et al., 2018) and have been validated in both long-term (1 year in Wang and Shprits (2019) and several years in Shprits et al. (2022)) and challenging event radiation belt simulations (Wang et al., 2020).

The new lifetime model covers all MLTs, which is a significant improvement comparing with previous lifetime models regarding the precipitation loss caused by chorus waves (e.g., Gu et al., 2012; Orlova & Shprits, 2014; Shprits et al., 2007). The calculated lifetime is valid for all MLT sectors, $\mathrm{Kp} \le 6$ and $L \in [3,6]$ and is provided to our community via data publication (Wang et al., 2022). To facilitate the usability of the presented model we provide the parameterization of the electron lifetime as polynomial functions of kinetic energy of electron and $L-$shell at each MLT and Kp in Wang et al. (2023). Using the new lifetime models can improve the agreement between simulations and observations. This new lifetime is very important for the calculation of MLT dependent precipitation, which is a crucial part of the magnetosphere-ionosphere-thermosphere coupling. The calculated and parametrized lifetime model presented in this paper has been tested using the VERB-4D code. By performing multiple simulations using the electron lifetime provided by the current study, Haas et al. (2023) revealed a missing dusk-side loss process in the Earth's ring current electrons. This lifetime model is also now used by the Multiscale Atmosphere-Geospace Environment Model (MAGE) code at the Center for Geospace Storms (CGS) and will be used in other models in future.

Acronyms

MLT Magnetic Local Time.

MLat Magnetic Latitude.

UBC Upper-band Chorus.

LBC Lower-band Chorus.

PA Pitch Angle.

EMFISIS Electric and Magnetic Field Instrument Suite and Integrated Science.

PP Plasmapause.

CRRES Combined Release and Radiation Effects Satellite.

THEMIS Time History of Events and Macroscale Interactions during Substorms.

R_E Earth Radii.

VERB-4D code four dimensional Versatile Electron Radiation Belt code.

Data Availability Statement

As stated in the paper, the calculated lifetime database is available for usage as a data publication (Wang et al., 2022). We also provide the coefficients of the polynomial fits of calculated electron lifetime in our data publication Wang et al. (2023). The full diffusion code (FDC) and the Versatile Electron Radiation Belt (VERB) code for the numerical simulations is available at this website: https://rbm.epss.ucla.edu/downloads/.

Acknowledgments

We would like to thank Hui Zhu for useful discussions. We are grateful to Melanie Burns and Karina Wilgan for the help with editing the paper. This project has received funding from the European Research Council (ERC) under the European Union's Horizon 2020 research and innovative programme (grant agreement number: 101124679 - WIRE). This project has received funding from the European Union's Horizon 2020 research and innovation programme under grant agreement No. 870452 (PAGER) and the Helmholtz-Gemeinshaft (HGF) [10.13039/501100001656]. Dedong Wang acknowledges the support from the Deutsche Forschungsgemeinschaft (DFG) through the project "Understanding the Properties of Chorus Waves in the Earth's Inner-magnetosphere and Their Effects on Van Allen Radiation Belt Electrons" (Chorus Waves) - WA 4323/5–1 (project number: 520916080). The Kp index was provided by GFZ Section 2.3 and downloaded from the World Data Center. The authors would also like to acknowledge the open access funding enabled and organized by the Projekt DEAL.

References

Agapitov, O., Mourenas, D., Artemyev, A., Mozer, F., Hospodarsky, G., Bonnell, J., & Krasnoselskikh, V. (2018). Synthetic empirical chorus wave model from combined Van Allen Probes and Cluster statistics. *Journal of Geophysical Research: Space Physics*, *123*(1), 297–314. https://doi.org/10.1002/2017JA024843

Albert, J. (2005). Evaluation of quasi-linear diffusion coefficients for whistler mode waves in a plasma with arbitrary density ratio. *Journal of Geophysical Research*, *110*(A3). https://doi.org/10.1029/2004JA010811

Albert, J., & Shprits, Y. (2009). Estimates of lifetimes against pitch angle diffusion. *Journal of Atmospheric and Solar-Terrestrial Physics*, *71*(16), 1647–1652. https://doi.org/10.1016/j.jastp.2008.07.004

Aseev, N. A., Shprits, Y. Y., Wang, D., Wygant, J., Drozdov, A. Y., Kellerman, A. C., & Reeves, G. D. (2019). Transport and loss of ring current electrons inside geosynchronous orbit during the 17 march 2013 storm. *Journal of Geophysical Research: Space Physics*, *124*(2), 915–933. https://doi.org/10.1029/2018JA026031

Bunch, N. L., Spasojevic, M., & Shprits, Y. Y. (2011). On the latitudinal extent of chorus emissions as observed by the polar plasma wave instrument. *Journal of Geophysical Research*, *116*(A4). https://doi.org/10.1029/2010JA016181

Cai, B., Wu, Y., & Tao, X. (2020). Effects of nonlinear resonance broadening on interactions between electrons and whistler mode waves. *Geophysical Research Letters*, *47*(11), e2020GL087991. Retrieved from https://doi.org/10.1029/2020GL087991

Drozdov, A. Y., Allison, H. J., Shprits, Y. Y., Elkington, S. R., & Aseev, N. A. (2021). A comparison of radial diffusion coefficients in 1-D and 3-D long-term radiation belt simulations. *Journal of Geophysical Research: Space Physics*, *126*(8), e2020JA028707. https://doi.org/10.1029/2020JA028707

Drozdov, A. Y., Shprits, Y., Aseev, N., Kellerman, A., & Reeves, G. D. (2017). Dependence of radiation belt simulations to assumed radial diffusion rates tested for two empirical models of radial transport. *Space Weather*, *15*(1), 150–162. https://doi.org/10.1002/2016SW001426

Glauert, S. A., Atkinson, J. W., Ross, J. P., & Horne, R. B. (2024). A new model of electron pitch angle distributions and loss timescales in the Earth's radiation belts. *Journal of Geophysical Research: Space Physics*, *129*, e2023JA032249. https://doi.org/10.1029/2023ja032249

Glauert, S. A., & Horne, R. B. (2005). Calculation of pitch angle and energy diffusion coefficients with the PADIE code. *Journal of Geophysical Research*, *110*(A4), A04206. https://doi.org/10.1029/2004JA010851

Gu, X., Shprits, Y. Y., & Ni, B. (2012). Parameterized lifetime of radiation belt electrons interacting with lower-band and upper-band oblique chorus waves. *Geophysical Research Letters*, *39*(15). https://doi.org/10.1029/2012GL052519

Haas, B., Shprits, Y. Y., Allison, H. J., Wutzig, M., & Wang, D. (2022). Which parameter controls ring current electron dynamics. *Frontiers in Astronomy and Space Sciences*, *166*. https://doi.org/10.3389/fspas.2022.911002

Haas, B., Shprits, Y. Y., Allison, H. J., Wutzig, M., & Wang, D. (2023). A missing dusk-side loss process in the terrestrial electron ring current. *Scientific Reports*, *13*(1), 970. https://doi.org/10.1038/s41598-023-28093-2

Horne, R., & Thorne, R. (2003). Relativistic electron acceleration and precipitation during resonant interactions with whistler-mode chorus. *Geophysical Research Letters*, *30*(10). https://doi.org/10.1029/2003GL016973

Kennel, C. F. (1969). Consequences of a magnetospheric plasma. *Reviews of Geophysics*, *7*(1–2), 379–419. https://doi.org/10.1029/rg007i001p00379

Kim, K.-C., Shprits, Y., Subbotin, D., & Ni, B. (2012). Relativistic radiation belt electron responses to GEM magnetic storms: Comparison of CRRES observations with 3-D VERB simulations. *Journal of Geophysical Research*, *117*(A8). https://doi.org/10.1029/2011JA017460

Li, W., Bortnik, J., Thorne, R., & Angelopoulos, V. (2011). Global distribution of wave amplitudes and wave normal angles of chorus waves using THEMIS wave observations. *Journal of Geophysical Research*, *116*(A12). https://doi.org/10.1029/2011JA017035

Li, W., Shprits, Y., & Thorne, R. (2007). Dynamic evolution of energetic outer zone electrons due to wave-particle interactions during storms. *Journal of Geophysical Research*, *112*(A10). https://doi.org/10.1029/2007JA012368

Li, W., Thorne, R., Angelopoulos, V., Bortnik, J., Cully, C. M., Ni, B., et al. (2009). Global distribution of whistler-mode chorus waves observed on the THEMIS spacecraft. *Geophysical Research Letters*, *36*(9). https://doi.org/10.1029/2009GL037595

Meredith, N. P., Horne, R. B., Thorne, R. M., & Anderson, R. R. (2003). Favored regions for chorus-driven electron acceleration to relativistic energies in the Earth's outer radiation belt. *Geophysical Research Letters*, *30*(16). https://doi.org/10.1029/2003GL017698

Meredith, N. P., Horne, R. B., Thorne, R. M., Summers, D., & Anderson, R. R. (2004). Substorm dependence of plasmaspheric hiss. *Journal of Geophysical Research*, *109*(A6). https://doi.org/10.1029/2004JA010387

Millan, R., & Baker, D. (2012). Acceleration of particles to high energies in Earth's radiation belts. *Space Science Reviews*, *173*(1–4), 103–131. https://doi.org/10.1007/s11214-012-9941-x

Ni, B., Thorne, R. M., Meredith, N. P., Horne, R. B., & Shprits, Y. Y. (2011). Resonant scattering of plasma sheet electrons leading to diffuse auroral precipitation: 2. Evaluation for whistler mode chorus waves. *Journal of Geophysical Research*, *116*(A4). https://doi.org/10.1029/2010JA016233

Ni, B., Thorne, R. M., Meredith, N. P., Shprits, Y. Y., & Horne, R. B. (2011). Diffuse auroral scattering by whistler mode chorus waves: Dependence on wave normal angle distribution. *Journal of Geophysical Research*, *116*(A10). https://doi.org/10.1029/2011JA016517

Orlova, K., & Shprits, Y. (2014). Model of lifetimes of the outer radiation belt electrons in a realistic magnetic field using realistic chorus wave parameters. *Journal of Geophysical Research: Space Physics*, *119*(2), 770–780. https://doi.org/10.1002/2013JA019596

Orlova, K., Shprits, Y., & Spasojevic, M. (2016). New global loss model of energetic and relativistic electrons based on van allen probes measurements. *Journal of Geophysical Research: Space Physics*, *121*(2), 1308–1314. https://doi.org/10.1002/2015JA021878

Ozeke, L. G., Mann, I. R., Murphy, K. R., Degeling, A. W., Claudepierre, S. G., & Spence, H. E. (2018). Explaining the apparent impenetrable barrier to ultra-relativistic electrons in the outer Van Allen belt. *Nature Communications*, *9*(1), 1844. https://doi.org/10.1038/s41467-018-04162-3

Reeves, G. D., McAdams, K. L., Friedel, R. H. W., & O'Brien, T. P. (2003). Acceleration and loss of relativistic electrons during geomagnetic storms. *Geophysical Research Letters*, *30*(10). https://doi.org/10.1029/2002GL016513

Ripoll, J.-F., Loridan, V., Cunningham, G. S., Reeves, G. D., & Shprits, Y. (2016). On the time needed to reach an equilibrium structure of the radiation belts. *Journal of Geophysical Research: Space Physics*, *121*(8), 7684–7698. https://doi.org/10.1002/2015JA022207

Sheeley, B., Moldwin, M., Rassoul, H., & Anderson, R. (2001). An empirical plasmasphere and trough density model: CRRES observations. *Journal of Geophysical Research*, *106*(A11), 25631–25641. https://doi.org/10.1029/2000JA000286

Shprits, Y. Y., Allison, H. J., Wang, D., Drozdov, A., Szabo-Roberts, M., Zhelavskaya, I., & Vasile, R. (2022). A new population of ultra-relativistic electrons in the outer radiation zone. *Journal of Geophysical Research: Space Physics*, *127*(5), e2021JA030214. https://doi.org/10.1029/2021JA030214

Shprits, Y. Y., Kellerman, A. C., Drozdov, A. Y., Spence, H. E., Reeves, G. D., & Baker, D. N. (2015). Combined convective and diffusive simulations: VERB-4D comparison with 17 march 2013 van allen probes observations. *Geophysical Research Letters*, *42*(22), 9600–9608. (Publisher: Blackwell Publishing Ltd). https://doi.org/10.1002/2015GL065230

Shprits, Y. Y., Li, W., & Thorne, R. M. (2006b). Controlling effect of the pitch angle scattering rates near the edge of the loss cone on electron lifetimes. *Journal of Geophysical Research*, *111*(A12). https://doi.org/10.1029/2006JA011758

Shprits, Y. Y., Meredith, N. P., & Thorne, R. M. (2007). Parameterization of radiation belt electron loss timescales due to interactions with chorus waves. *Geophysical Research Letters*, *34*(11). https://doi.org/10.1029/2006GL029050

Shprits, Y. Y., Subbotin, D., & Ni, B. (2009). Evolution of electron fluxes in the outer radiation belt computed with the VERB code. *Journal of Geophysical Research*, *114*(A11). https://doi.org/10.1029/2008JA013784

Shprits, Y. Y., Subbotin, D. A., Meredith, N. P., & Elkington, S. R. (2008). Review of modeling of losses and sources of relativistic electrons in the outer radiation belt II: Local acceleration and loss. *Journal of Atmospheric and Solar-Terrestrial Physics*, *70*(14), 1694–1713. https://doi.org/10.1016/j.jastp.2008.06.014

Shprits, Y. Y., Thorne, R. M., Horne, R. B., & Summers, D. (2006). Bounce-averaged diffusion coefficients for field-aligned chorus waves. *Journal of Geophysical Research*, *111*(A10). https://doi.org/10.1029/2006JA011725

Spasojevic, M., & Shprits, Y. (2013). Chorus functional dependencies derived from CRRES data. *Geophysical Research Letters*, *40*(15), 3793–3797. https://doi.org/10.1002/grl.50755

Subbotin, D., Shprits, Y., & Ni, B. (2010). Three-dimensional verb radiation belt simulations including mixed diffusion. *Journal of Geophysical Research*, *115*(A3). https://doi.org/10.1029/2009JA015070

Subbotin, D., Shprits, Y., & Ni, B. (2011). Long-term radiation belt simulation with the VERB 3-D code: Comparison with CRRES observations. *Journal of Geophysical Research*, *116*(A12). https://doi.org/10.1029/2011JA017019

Summers, D. (2005). Quasi-linear diffusion coefficients for field-aligned electromagnetic waves with applications to the magnetosphere. *Journal of Geophysical Research*, *110*(A8). https://doi.org/10.1029/2005JA011159

Summers, D., & Thorne, R. M. (2003). Relativistic electron pitch-angle scattering by electromagnetic ion cyclotron waves during geomagnetic storms. *Journal of Geophysical Research*, *108*(A4). https://doi.org/10.1029/2002JA009489

Tao, X., Bortnik, J., Albert, J. M., Liu, K., & Thorne, R. M. (2011). Comparison of quasilinear diffusion coefficients for parallel propagating whistler mode waves with test particle simulations. *Geophysical Research Letters*, *38*(6). https://doi.org/10.1029/2011GL046787

Thorne, R. M. (2010). Radiation belt dynamics: The importance of wave-particle interactions. *Geophysical Research Letters*, *37*(22). https://doi.org/10.1029/2010GL044990

Thorne, R. M., O'Brien, T., Shprits, Y., Summers, D., & Horne, R. B. (2005). Timescale for MeV electron microburst loss during geomagnetic storms. *Journal of Geophysical Research*, *110*(A9). https://doi.org/10.1029/2004JA010882

Tu, W., Li, W., Albert, J. M., & Morley, S. K. (2019). Quantitative assessment of radiation belt modeling. *Journal of Geophysical Research: Space Physics*, *124*, 898–904. https://doi.org/10.1029/2018ja026414

Wang, D., Shprits, Y., & Haas, B. (2022). Lifetime of energetic electrons due to interactions with chorus waves. [dataset]. https://doi.org/10.5880/GFZ.2.7.2022.002. *GFZ Data Services*

Wang, D., Shprits, Y., Michaelis, I., & Haas, B. (2023). The 3-rd order polynomial fit coefficients of electron lifetime caused by interaction with chorus waves. [dataset]. https://doi.org/10.5880/GFZ.2.7.2023.008. *GFZ Data Services*

Wang, D., & Shprits, Y. Y. (2019). On how high-latitude chorus waves tip the balance between acceleration and loss of relativistic electrons. *Geophysical Research Letters*, *46*(14), 7945–7954. https://doi.org/10.1029/2019GL082681

Wang, D., Shprits, Y. Y., Zhelavskaya, I. S., Agapitov, O. V., Drozdov, A. Y., & Aseev, N. A. (2019). Analytical chorus wave model derived from van allen probe observations. *Journal of Geophysical Research: Space Physics*, *124*(2), 1063–1084. https://doi.org/10.1029/2018JA026183

Wang, D., Shprits, Y. Y., Zhelavskaya, I. S., Effenberger, F., Castillo, A. M., Drozdov, A. Y., et al. (2020). The effect of plasma boundaries on the dynamic evolution of relativistic radiation belt electrons. *Journal of Geophysical Research: Space Physics*, *125*(5), e2019JA027422. https://doi.org/10.1029/2019ja027422

Wong, J.-M., Meredith, N. P., Horne, R. B., Glauert, S. A., & Ross, J. P. (2024). New chorus diffusion coefficients for radiation belt modeling. *Journal of Geophysical Research: Space Physics*, *129*(1), e2023JA031607. https://doi.org/10.1029/2023ja031607

Xiao, F., Su, Z., Zheng, H., & Wang, S. (2009). Modeling of outer radiation belt electrons by multidimensional diffusion process. *Journal of Geophysical Research*, *114*(A3). https://doi.org/10.1029/2008JA013580

Zhu, H., Shprits, Y. Y., Spasojevic, M., & Drozdov, A. Y. (2019). New hiss and chorus waves diffusion coefficient parameterizations from the Van Allen Probes and their effect on long-term relativistic electron radiation-belt VERB simulations. *Journal of Atmospheric and Solar-Terrestrial Physics*, *193*, 105090. https://doi.org/10.1016/j.jastp.2019.105090